

# Simultaneous predictive bands for functional time series using minimum entropy sets

Nicolás Hernández<sup>a</sup>, Jairo Cugliari<sup>b,\*</sup>, Julien Jacques<sup>b</sup>

<sup>a</sup>*MRC Biostatistics Unit, University of Cambridge, UK*

<sup>b</sup>*Université de Lyon, Lyon 2, ERIC UR 3083*

---

## Abstract

Functional Time Series are sequences of dependent random elements taking values on some functional space. Most of the research on this domain is focused on producing a predictor able to forecast the value of the next function having observed a part of the sequence. For this, the Autoregressive Hilbertian process is a suitable framework. We address here the problem of constructing simultaneous predictive confidence bands for a stationary functional time series. The method is based on an entropy measure for stochastic processes, in particular functional time series. To construct predictive bands we use a functional bootstrap procedure that allow us to estimate the prediction law through the use of pseudo-predictions. Each pseudo-realisation is then projected into a space of finite dimension, associated to a functional basis. We use Reproducing Kernel Hilbert Spaces (RKHS) to represent the functions, considering then the basis associated to the reproducing kernel. Using a simple decision rule, we classify the points on the projected space among those belonging to the minimum entropy set and those that do not. We push back the minimum entropy set to the functional space and construct a band using the regularity property of the RKHS. The proposed methodology is illustrated through artificial and real-world data sets.

**Keywords:** Functional time series, Autoregressive Hilbertian process, RKHS, Bootstrap, Entropy, Predictive bands.

---

## 1. Introduction

While Functional Data Analysis (FDA) [Ramsay \(2006\)](#) cope with independent and identical distributed realizations of functional data, the term Functional Time Series (FTS) refers to dependent series of random elements lying in some functional space. Besides the academic research interest of such an elegant framework, FTS have important practical usefulness. In some cases, they allow one to consider an alternative modelling scheme to classical time series thanks to its ability to intrinsically deal with non stationary pattern such as seasonality. Moreover, they can be of great help if one has a heterogeneous sampling scheme where records are observed at unequally spaced time points.

A simple yet powerful device to construct a FTS is proposed by [Bosq \(2000\)](#). The idea is to take slices of an underlying continuous stochastic process, say  $\xi = \{\xi(t); t \in \mathbb{R}\}$ , using a window of fixed size  $\delta > 0$ . Then, we consider the FTS  $Z$  such that  $Z_k(t) = \xi((k-1)\delta + t); k \in \mathbb{Z}$  with  $t \in (0, \delta)$ . In many real-world applications this scheme is reasonable: an underlying phenomenon of continuous nature exists even if data is recorded at some sampling rate. Examples of this can be found in electrical devices monitor ([Bonnevay et al., 2019](#)), energy demand ([Antoniadis et al.,](#)

---

\*Email: Jairo.Cugliari@univ-lyon2.fr

2016), air pollution (Papadimitis and Shang, 2020) or geology (Hörmann et al., 2010) among others. Notice that the device is particularly fruitful if the quantity  $\delta$  is tailored to some seasonal component of the series  $\xi$ . In such cases, the series  $Z$  naturally incorporates the non stationary pattern induced by the seasonality. Other kinds of FTS involves more general situations, as for instance sequences of functions that does not verify continuity constraints between consecutive functions (see Aue et al. (2015)).

One important task related to FTS is forecasting. That is, after having observed  $n$  realizations of the process  $Z$ , say  $Z_1, \dots, Z_n$ , the aim is to predict the next whole function  $Z_{n+1}(t)$ ,  $t \in (0, \delta)$ . Autoregressive Hilbertian processes (ARH) are the natural extension of univariate autoregressive processes to the functional data framework where Hilbert spaces are considered. The term Functional Autoregressive (FAR) is sometimes also used to name the same process, while this can produce confusion with univariate autoregressive non linear processes. In a nutshell, they consist in linking two consecutive functions of a stationary FTS through a linear operator plus a functional noise. Since the functions are usually supposed to take values on some Hilbert space, the processes are also named autoregressive Hilbertian (ARH). An excellent review of these processes can be found in Alvarez-Liéban (2017). Several works address the problem of predicting the function  $Z_{n+1}(t)$  at the moment  $n$  using variants of ARH (Aue et al., 2015; Nagbe et al., 2018; Wang et al., 2020) or in a more general framework such as non linear version of FTS (Antoniadis et al., 2006).

While point-wise prediction gives helpful information about the future evolution of FTS, uncertainty quantification is often needed to produce valid inference. Estimating the predictive law has received much less attention in the FTS literature. In general, bootstrap methods are used to produce pseudo predictions. Then, some kind of central region is taken to be the predictive band. For instance, Hyndman and Shang (2009) describe the FTS as a set of univariate time series associated to projected components. Then, using classical time series tools produce individual predictions and pseudo predictions based on a residual bootstrap. The univariate pseudo predictions are pushed back to the functional space to obtain functional pseudo predictions. With this, the band is constructed pointwisely taking the quantiles at some coverage level. Antoniadis et al. (2012) use a non linear version of FTS where the predictor is a weighted mean of functions with weights increasing with the similarity between the last observed function and every function in the dataset. The set of weights is the key element of the bootstrap procedure since the more a function is similar with the current one, the more likely the chances of its next function are to be sampled. The band is constructed using heuristics coming from econometric literature. In Papadimitis and Shang (2020) the authors propose a model-free bootstrap procedure based on the prediction generated by a VAR model applied to Karhunen–Loève coefficients of the FTS. Then simultaneous and pointwise intervals for the prediction are constructed using the bootstrap studentized prediction error.

In this paper we address the problem of constructing a confidence band for the prediction of the FTS. The aim is to construct a region  $\mathcal{B}_{n+1}^{1-\alpha}$  which covers the function  $Z_{n+1}(t)$ , that is  $P(Z_{n+1}(t) \in \mathcal{B}_{n+1}^{1-\alpha}) \geq 1 - \alpha$  for a fixed risk level  $\alpha \in (0, 1)$ . The probability measure is the one induced by the information available at the moment  $n$ . Notice that this prediction band requires simultaneously coverage of the whole curve  $Z_{n+1}(t)$ , which in general is a difficult requirement, see Degras (2017) for a discussion in the functional data context. Since it is usual to represent functions by the projection coefficients over a basis, some works explored the option of constructing a confidence region on the coefficients space (Antoniadis et al., 2006, 2012). However, obtaining simultaneous confidence bands sometimes requires additional regularity assumptions on the function spaces (Genovese and Wasserman, 2005).

Probability densities play an important role in the construction of predictive intervals. However, for functional data the concept of density cannot be well-defined (Delaigle et al., 2010) in the func-

tional space. In this sense, as the usual workflow is to deal with the projected coefficients of the functions in some basis, the authors propose to consider the probability density in such multivariate space. An option to sort this out is the use of some metric (distance) to infer the probability law behind the generation of the functions. This metric can be a depth function, (Fraiman and Muniz (2001); López-Pintado and Romo (2009); Cuevas et al. (2007) among others); a distance (Galeano et al. (2015); Martos et al. (2014); Cardot et al. (2013) and references therein); or an information theory tool such as entropy, Martos et al. (2018). These three concepts are linked in the sense that they induce an order in a functional data set and allow constructing  $(1 - \alpha)$ -central regions in the original space where the functions inhabit. Ideally, the main condition that these  $(1 - \alpha)$ -central regions should satisfy is that they concentrate a high amount (at least  $1 - \alpha$ , with  $\alpha \in [0, 1]$ ) of probability inside. In multivariate spaces, these  $(1 - \alpha)$ -central regions are known in the literature as high density regions (HDR), see Hyndman (1996).

In this paper we propose to use Minimum-Entropy-Sets (MES) as a way to estimate the HDR of the predictive law of the projection coefficients to then construct prediction bands. Our procedure can be used on top of any FTS forecasting approach, providing a predictor and a bootstrap method. Additional regularity of the functional space may be required to be push back the MES to the functional space. Our choice is to work on the special case of Hilbert spaces given by reproducing kernels (RKHS) that ensures the continuity of the pointwise evaluation functional.

The paper is organized as follows: In section 2 we present the RKHS framework needed for representing the ARH processes in such spaces, as well as considerations about the simulation, estimation and prediction procedures. We focus on predictive inference in section 3, defining Minimum-Entropy-Sets, a bootstrap procedure compatible with FTS and the predictive confidence bands methodology. Section 4 describes the experimental design using Monte Carlo simulation to show the good covering results of our proposal and a real-world data application. We conclude the paper with section 5.

## 2. The autoregressive Hilbertian model: ARH

In this section we introduce notation and recall well-known facts about representing a function with Reproducing Kernel Hilbert Spaces (RKHS) and autoregressive Hilbert (ARH) processes. All the random elements below are defined in the same probability space  $(\Omega, \mathcal{F}, P)$ .

### 2.1. Representing functional data using RKHS

In general we cannot observe the full trajectories of functional variables realisations. Since it is also the case for FTS, our input data is the set of discrete and noisy trajectories that constitutes realisations of the functional variable, also known in the literature as raw functional data (Hsing and Eubank, 2015). In what follows we set the functional space  $\mathcal{H} \subset L_2[T]$  the space of (classes of) square-integrable functions over the compact  $T$ . In our case we set  $T = [0, \delta]$ , with  $\delta = 1$  without loss of generality. In that sense, raw functional data consist of the collection of the functions recorded over a grid of  $m$  discretized points, say  $t_1, \dots, t_m$  (usually equally spaced). The analysis departs from a collection of discrete functions, hereafter curves:  $\{z_j(t_i)\}_{i=1}^m$  for  $j = 1, \dots, n$ .

As is usual in the functional data literature, in order to estimate the underlying functional object that generated each realisation  $z_j$  we need to choose a system of orthonormal basis functions. Following the approach in Muñoz and González (2010), we propose to chose  $\mathcal{H} = \mathcal{H}_K$  as a RKHS, such that the family of basis functions  $\Phi = \{\phi_1, \dots, \phi_d\}$  generates the functional subspace  $\mathcal{H}_K$  through its linear span. These basis functions are linked to the positive-semidefinite kernel function  $K = K(s, t)$

associated to  $\mathcal{H}_K$ . Any realization  $z(t)$  can be approximated by the following functional estimator

$$\tilde{z}(t) := \arg \min_{f \in \mathcal{H}} \sum_{i=1}^m L(z(t_i), f(t_i)) + \gamma \|f\|_{\mathcal{H}}^2, \quad (1)$$

where  $\gamma > 0$  is a regularization parameter,  $\|f\|_{\mathcal{H}}$  is the norm of the function  $f$  in  $\mathcal{H}$  and  $L(w, z) = (w - z)^2$  is a loss function. By the Representer Theorem (Cucker and Smale, 2002, Theorem 5.2, p. 91) the solution of the problem stated in Eq. (1) exists, is unique, and admits the following representation

$$\tilde{z}(t) = \sum_{i=1}^m a_i K(t, t_i) = \mathbf{a}^T \mathbf{K}_t, \quad (2)$$

where  $\mathbf{K}_t = \{K(t_1, t), \dots, K(t_m, t)\}$  is the vector of kernel evaluations and the linear combination coefficients  $\mathbf{a} = (a_1, \dots, a_m) \in \mathbb{R}^m$  are obtained as the solution the linear system  $(\gamma \mathbf{I}_m + \mathbf{K})\mathbf{a} = \mathbf{z}$ , for  $\mathbf{z} = (z(t_1), \dots, z(t_m))^T$ ,  $\mathbf{I}_m$  an  $m \times m$  identity matrix, and  $\mathbf{K}$  the Gram matrix with the kernel function evaluations over the grid  $t_1, \dots, t_m$ . Now, we use the Mercer decomposition theorem (J Mercer, 1909) to obtain the basis. Indeed, since  $K$  is a positive-definite and symmetric kernel function with associated integral operator  $I_K(z) = \int_T K(\cdot, t)z(t)dt$ , it admits a spectral decomposition into a sequence  $(\lambda_i, \phi_i)_{i \geq 1}$  of eigenvalue-eigenfunction pairs. Then, each estimated functional datum  $\tilde{z}(t)$  in the sample can be expressed as follows

$$\tilde{z}(t) = \sum_{i=1}^m c_i \phi_i(t), \quad (3)$$

where  $c_i$  are the projection coefficients of  $\tilde{z}(t)$  onto the space generated by the eigenfunctions  $\phi_i$ . Nevertheless, the expression in Eq. (3) is an unhelpful representation when the sequence of eigenpairs  $(\lambda_i, \phi_i)_{i \geq 1}$  is unknown. With the sample data at hand  $c_i$  can be estimated by:

$$\hat{c}_i = \frac{l_i}{\sqrt{m}} (\mathbf{a}^T \mathbf{v}_i), \quad (4)$$

where  $(l_i, \mathbf{v}_i)$  are the  $i^{\text{th}}$  eigenvalue (in decreasing order) and eigenvector of  $\mathbf{K}$ . It is possible to approximate the development in Eq. (4) by truncating the sum by the first few terms. Therefore, we represent each function  $z(t)$  with a finite representation in  $\mathbb{R}^d$  given by  $\hat{\mathbf{c}} = \{\hat{c}_1, \dots, \hat{c}_d\}$ , where  $d \leq \text{rank}(\mathbf{K})$ .

## 2.2. Autoregressive Hilbert process

Following the previous notation, the sequence  $Z = \{Z_k, k \in \mathbb{Z}\}$  of random functions on  $\mathcal{H}$  follows an ARH(1) if,

$$Z_k = \mu + \Psi(Z_{k-1} - \mu) + \epsilon_k, \quad (5)$$

where  $\mu$  is the mean function,  $\Psi$  is a linear bounded (continuous) operator on  $\mathcal{H} \mapsto \mathcal{H}$  and  $\epsilon = \{\epsilon_k, k \in \mathbb{Z}\}$  a strong white noise in  $\mathcal{H}$  such that  $\mathbb{E}\|\epsilon_k\| < \infty$  and  $E[Z_0] = \mu$ ,  $E\|Z_0\|^2 < \infty$ . Under mild conditions, the expression defined in Eq. (5) defines a strictly stationary stochastic process in  $\mathcal{H}$ . Given  $Z_1, \dots, Z_n$ , the best predictor of the function  $Z_{n+1}$  in the mean-square-error sense is given by

$$\tilde{Z}_{n+1} = \mathbb{E}[Z_{n+1} | Z_1, \dots, Z_n], \quad (6)$$

which results for the ARH process in  $\tilde{Z}_{n+1} = \mu + \Psi(Z_n - \mu)$ . This predictor is not statistical in nature because it depends on parameters of the unknown probability law. Therefore, one needs to estimate  $\mu$  and  $\Psi$  to get a statistical predictor. A simple way is to use the empirical counterpart of the population

mean to estimate the mean function. The estimation of  $\Psi$  is more cumbersome because it involves unbounded operators. For this, the cross-covariance operator of lag  $r$  is defined as

$$\Gamma_r = \mathbb{E}[(Z_0 - \mu) \otimes (Z_r - \mu)], \quad (7)$$

which under mild conditions is a trace-class operator. To estimate the operator  $\Psi$  we use the covariance operator ( $\Gamma_0$ ) and the cross-covariance operator ( $\Gamma_1$ ), related by a Yule-Walker like expression:

$$\Gamma_0 \Psi = \Gamma_1. \quad (8)$$

If  $\mathcal{H}$  is of finite dimension, then one can just plug in the empirical counterparts of  $\Gamma_0$  and  $\Gamma_1$  and solve to obtain  $\Psi$ . However, in the general case the unboundedness of the inverse of  $\Gamma_0$  implies that the expression in Eq. 8 is an ill-posed problem, see [Mas and Pumo \(2011\)](#) for a detailed discussion. Fortunately, the problem has more impact for the development of theoretical results. The empirical equivalents of the operators are matrices and one relies on regularized versions of the inverse of the covariance matrix to obtain the estimation of  $\Psi$ . A second important property of ARH processes is worth to mention since it is used for simulation. Indeed, if  $Z$  follows an ARH(1) then

$$\Gamma_\epsilon = \Gamma_0 - \Psi \Gamma_0 \Psi^T, \quad (9)$$

where  $\Gamma_\epsilon$  is the covariance operator of  $\epsilon$  ([Bosq, 2000](#), Chap 3.). This means that only two of the three operators can be chosen freely for the simulation of ARH trajectories. Moreover, since  $\Gamma_\epsilon$  needs to be positive definite, not every couple of  $\Psi$  and  $\Gamma_0$  will produce a compatible innovation process  $\epsilon$ .

*Estimation and prediction.* In practice, only finite measurements on each function are used to estimate the parameter. Given the finite, truncated representation of each curve in Eq. 3 and the estimated coefficients,  $\hat{c}_i$ , the mean function can be estimated by

$$\hat{\mu}(t) = \sum_{i=1}^d \tilde{c}_i \phi_i(t), \quad \text{with } \tilde{c}_i = \frac{1}{n} \sum_{k=1}^n \hat{c}_{k,i}. \quad (10)$$

As it is usual in FDA the operations concerns the projection coefficients, which are then expanded on the basis constructed using a kernel function. Similarly, the corresponding covariance  $\hat{\Gamma}_0$  and cross-covariance  $\hat{\Gamma}_1$  estimators of the operators  $\Gamma_0$  and  $\Gamma_1$  are

$$\hat{\Gamma}_r = \frac{1}{n-r} \sum_{k=1}^{n-r} \sum_{i'=1}^d \sum_{i=1}^d \hat{d}_{k,i} \hat{d}_{k,i'+r} \phi_i \otimes \phi_{i'}, \quad r = 0, 1, \quad (11)$$

where  $\hat{d}_{k,i} = \hat{c}_{k,i} - \tilde{c}_i$ . Notice that the coefficients can be arranged into two squared  $d \times d$  matrices, say  $\hat{\mathbf{C}}_0$  and  $\hat{\mathbf{C}}_1$ ,

$$(\hat{\mathbf{C}}_r)_{i,i'} = \frac{1}{n-r} \sum_{k=1}^{n-r} \hat{d}_{k,i} \hat{d}_{k,i'+r}, \quad r = 0, 1. \quad (12)$$

At this point, one can estimate the projection coefficients of  $\Psi$  on the double basis induced by the kernel. For this, we solve the equivalent of Eq. (8) to obtain  $\hat{\mathbf{P}} = \hat{\mathbf{C}}_0^{-1} \hat{\mathbf{C}}_1$ . Notice that the truncation introduced in Section 2.1 sized down these matrices to  $d < m$ . Besides the trivial reduction on the computation times of these matrices, the truncation induces a regularization effect needed to better approximate the operator  $\Psi$  (see [Bosq \(2000\)](#)). Finally,  $\Psi$  is estimated by:

$$\hat{\Psi} = \sum_{i'=1}^d \sum_{i=1}^d \hat{p}_{i,i'} \phi_i \otimes \phi_{i'}, \quad (13)$$

where  $\hat{p}_{i,i'} = (\hat{\mathbf{P}})_{i,i'}$ . The one-step-ahead prediction  $\hat{Z}_{n+1|n}$  is obtained by applying  $\hat{\Psi}$  to the last observed function.

*Simulation.* Generation of a sequence of  $n$  realizations  $Z_1, \dots, Z_n$  of a function-valued regressive stochastic process is studied in [Damon and Guillas \(2005\)](#). The problem is not trivial since an ARH processes has a rich second-order structure that imposes restrictions between the autoregression and covariance operators (of the process and its innovation). The authors argue that simulating in finite space is more rationale. Then, a natural choice is to project the functions and the operators in some finite space  $\mathcal{H}_{m'}$  of dimension  $m' < m$ . To disconnect our estimation procedure from the simulation scheme, we use a Fourier basis in our experiments. The functional nature of the simulated curves is obviously enhanced with increasing values of  $m'$ . The simulation scheme goes as follows.

1. Choose the vector or matrix representation of  $\mu, \Psi$ , and  $\Gamma_0$  on the space  $\mathcal{H}_{m'}$ .
2. Obtain the compatible matrix representation of  $\Gamma_\epsilon$  using Eq. (9). If it is not possible, then the chosen  $\Psi$  and  $\Gamma_0$  are incompatible with an ARH process.
3. Simulate an i.i.d. sequence  $(\xi_k)$  of random variables in  $\mathcal{H}_{m'}$ , and use the transformation  $\epsilon_k = \Gamma_0^{1/2} \xi_k, k = 0, 1, \dots, n$  to obtain the compatible innovation process.
4. Set  $Z_0 = \epsilon_0$ , then use the recursion in Eq. (5) to generate the values  $Z_1, \dots, Z_n$ .

### 3. Making predictive inference with the ARH-RKHS model

Prediction is one of the main objectives in time series analysis. In terms of uncertainty, prediction intervals bring more information about the future values of a random variable than point forecasts. In that sense, prediction intervals entail a set of values that the realisation of the future random variable could take, conditional on past information and given a certain probability. In the functional time series context, given the functional nature of the observations, the predictive confidence intervals take the form of predictive confidence bands (PCB), which implies the definition of a bounded region in the original space where the functions inhabit, such that if we randomly take one realisation of the sample of functional time series, it will be fully enclosed by the band with a given probability.

We define the lower and upper functional statistics,  $L_{n+1|n}(t)$  and  $U_{n+1|n}(t)$  both in  $\mathcal{H}$  such that the region comprised by  $\{[L_{n+1|n}(t), U_{n+1|n}(t)] : t \in T\}$  fully contains the conditional expectation  $\tilde{Z}_{n+1|n}$  (see Eq. (6)) with a probability of  $1 - \alpha$ .

**Definition 1.** Let  $L_{n+1|n}(t)$  and  $U_{n+1|n}(t)$  be two elements of  $\mathcal{H}$ . We define a predictive band as the set  $\mathcal{B}_{n+1|n}^{1-\alpha} = \{(t, z) \in R^2 : L_{n+1|n}(t) \leq z \leq U_{n+1|n}(t), t \in T\}$  such that

$$P(\tilde{Z}_{n+1|n} \in \mathcal{B}_{n+1|n}^{1-\alpha}, \forall t \in T) \geq 1 - \alpha. \quad (14)$$

Following [Degras \(2017\)](#), there are at least two options to conduct predictive inference in the functional context: i) pointwisely or ii) simultaneously. Under the pointwise estimation of  $\mathcal{B}^{1-\alpha}$  the condition stated in Eq. 14 is satisfied for each  $t \in T$ , independently. Let say the prediction is sampled at  $m$  points in the domain  $T$ , then the pointwise confidence band,  $\widehat{\mathcal{B}}_{n+1|n}^{x,p}$  is constructed by the concatenation of  $m$  prediction intervals  $[L_{n+1|n}^p(t_i), U_{n+1|n}^p(t_i)]$  for each  $t_i$ , with  $i = 1, \dots, m$ . The independent assumption implies that the joint probability is equal to the multiplication of the marginal probabilities for each  $t_i$ , then

$$P(L_{n+1|n}^p(t_i) \leq \tilde{Z}_{n+1|n}(t_i) \leq U_{n+1|n}^p(t_i), \forall i = 1, \dots, m) = (1 - \alpha)^m \leq (1 - \alpha),$$

which does not satisfy the condition stated in Eq. 14 (unless trivial cases). Even though the pointwise predictive bands are a valid inferential method, in general their coverage is less than  $1 - \alpha$ , which can mislead the conclusion in terms of the confidence of the prediction, see [Degras \(2017\)](#) for a deeper



discussion. To ensure that the condition stated in Eq. 14 is satisfied, which means that the coverage of the band is at least  $1 - \alpha$  for the entire domain, we need to tackle this problem under a simultaneous approach. Our choice is to approximate  $\mathcal{B}_{n+1|n}^{1-\alpha}$  using  $1 - \alpha$  minimum entropy sets on the  $d$ -dimensional representation space of functions as defined in Section 2.1.

### 3.1. $1 - \alpha$ minimum entropy sets

In this paper we consider an information theory criteria of minimum entropy. The entropy of a random variable gives information about the uncertainty associated to its realizations. Let  $\mathbf{c} \in \mathbb{R}^d$  a real-valued vector with continuous density function  $f_C$ , then the  $\nu$ -entropy (see Rényi et al. (1961)) of a set  $A \subset \mathbb{R}^d$  is given by

$$H_\nu(A) = \frac{1}{1 - \nu} \log \left( \int_A f_C^\nu(\mathbf{c}) d\mathbf{c} \right), \quad (15)$$

for  $\nu > 0$  and  $\nu \neq 1$ . Following Martos et al. (2018) we define  $\mathcal{R}_{1-\alpha}$  as the  $1 - \alpha$  minimum entropy set (MES) for the variable  $C$  as follows:

$$\mathcal{R}_{1-\alpha}(C) := \{\arg \min_{A \subset \mathbb{R}^d} H_\nu(A) \text{ s.t. } P(A) \geq 1 - \alpha\}. \quad (16)$$

The MES can be obtained using a local version of the entropy in Eq. (15). Given a proximity parameter  $\delta > 0$ , we consider the  $\delta$ -local  $\nu$ -entropy for the point  $\mathbf{c}$  as  $H_\nu(A)$  where  $A = \Delta_{\mathbf{c}}$  is a ball  $B$  centred at  $\mathbf{c}$  with radius  $r_\delta$ , such that  $\delta = \int_B f_C(\mathbf{c}) d\mathbf{c}$ . Given a set of data points  $C_n = \{\mathbf{c}_1, \dots, \mathbf{c}_n\} \in \mathbb{R}^d$ , the local entropy induces an order since it computes a univariate measure for each data point. The local entropy for the data at hand is obtained using the estimator  $\widehat{H}_\nu(\Delta_{\mathbf{c}_i}) = \exp(\bar{d}_k(\mathbf{c}_i, C_n))$ , where  $\bar{d}_k(\mathbf{c}_i, C_n)$  is the average distance from  $\mathbf{c}_i$  to its  $k$ -th-nearest neighbours in  $C_n$ .

Then, a binary decision rule can be used to define whether a point belongs to the MES or not by simply taking the points that are below the  $1 - \alpha$  quantile of the sets of estimated local entropies. This rule is theoretically justified in Muñoz and Moguerza (2006), where the authors define a non-parametric estimator for this region using a One-Class Neighbour Machine problem. The idea is to construct a binary classifier that separates a given set of realisations of  $C$  between those belonging to the  $1 - \alpha$  MES and those that do not. The classifier provides the same decision rule  $D$  as before, that is  $D(\mathbf{c}) = 1$  if  $\mathbf{c}$  corresponds to the  $1 - \alpha$  proportion of elements that belongs to a low entropy (high density) region and zero otherwise. Martos et al. (2018) proved that the proposed estimator asymptotically converges to the true  $\mathcal{R}_{1-\alpha}$  as the sample size increases.

### 3.2. Bootstrap procedure for FTS

One important issue when constructing prediction intervals or regions, is the assumption made with respect to the distribution of the innovations of the process. The standard approach is to assume Gaussian innovations, which generate prediction intervals centred on the conditional expectation function, and in general do not constitute a good probabilistic framework when dealing with real time series data. Hence, some alternative approach should be used to address this issue.

In that context the bootstrap technique arose, as a method that allows to get an approximation of the estimator distribution throughout drawing random samples from the empirical distribution function. When dealing with time dependent data such as functional time series, the usual bootstrap techniques lead to inconsistent statistics. There are several methodologies oriented to tackle this problem and proposed bootstrap techniques for FTS, see Shang (2018); Paparoditis et al. (2018); Chen and Pun (2019); Franke and Nyarige (2019).

In this paper we consider an extension to the functional context of the residual bootstrap methodology proposed by Pascual et al. (2004) for univariate autoregressive models and extended to the

multivariate framework by [Fresoli et al. \(2014\)](#). In the FTS context, [Franke and Nyarige \(2019\)](#) give a formal derivation of this procedure and study the statistical properties of the bootstrapped estimators. They also prove that the method provides asymptotically valid estimates of the mean function and covariance operator as well as the convergence of the empirical distribution of the centered innovations.

Given  $Z_1, \dots, Z_n$  that follow an ARH(1) process as in Eq. (5) the functional residual bootstrap procedure is as follows.

1. Obtain the full sample estimators  $\hat{\mu}$  and  $\hat{\Psi}_K$  using the  $n$  realizations;
2. estimate the fitted values  $\hat{Z}_k = \hat{\mu} + \hat{\Psi}_K(Z_{k-1} - \hat{\mu})$  with a functional model with  $k = 2, \dots, n$ ;
3. obtain the residuals:  $\hat{\epsilon}_k^\dagger = \hat{Z}_k - Z_k$  and centre them by subtracting the mean  $\hat{\epsilon}_k = \hat{\epsilon}_k^\dagger - \bar{\epsilon}_k^\dagger$ ;
4. for  $b = 1, \dots, B$ ,
  - (a) obtain  $\hat{\epsilon}_k^*$  by resampling with replacement from  $\hat{\epsilon}_k$ , and construct the functional bootstrap series  $Z_k^* = \Psi_K^*(Z_{k-1}) + \hat{\epsilon}_k^*$  fixing the first initial curve  $Z_1^* = Z_1$ ;
  - (b) with  $Z_1^*, \dots, Z_n^*$  obtain  $\hat{\Psi}_K^*$ ;
  - (c) obtain the  $h$  step ahead forecast  $\widehat{Z}_{n+h|n}^* = \hat{\Psi}_K^*(Z_{n-1+h|n})$ , conditioning on the original FTS and store  $\widehat{Z}_{n+h|n}^{(b)} := \widehat{Z}_{n+h|n}^*$ .

At the end of the procedure, we have  $B$  bootstrap predictive pseudo-replicates  $\widehat{Z}^* = \{\widehat{Z}_{n+h|n}^{(1)}, \dots, \widehat{Z}_{n+h|n}^{(B)}\}$  that follow the predictive law of  $Z_n$  as shown in [Franke and Nyarige \(2019\)](#).

### 3.3. Constructing the predictive confidence bands

Now we are able to define the simultaneous  $\text{PCB}_{1-\alpha}$  for a given one-step-ahead functional prediction  $\widehat{Z}_{n+1|n}$  as predictive confidence bands with probability  $1 - \alpha$ . At this stage it is important to recall that in the functional context a point prediction refers to the prediction of the whole function. Let  $\mathbf{c} = \{\mathbf{c}_d^{(1)}, \dots, \mathbf{c}_d^{(B)}\} \in \mathbb{R}^d$  be the RKHS multivariate representation of  $\widehat{Z}^*$  as defined in Section 2.1. With this, we can estimate the minimum entropy set  $\widehat{\mathcal{R}}_{1-\alpha}(\mathbf{c})$  from Eq. 16 using the classifier of [Martos et al. \(2018\)](#). Consider the set of indices corresponding to the functions whose multivariate RKHS representation is associated to  $\widehat{\mathcal{R}}_{1-\alpha}(\mathbf{c})$ , formally  $\mathcal{A} = \{b \in \{1, \dots, B\} : \mathbf{c}_d^{(b)} \in \widehat{\mathcal{R}}_{1-\alpha}(\mathbf{c})\}$ . Using this we estimate the  $\text{PCB}_{1-\alpha}$  for  $\widehat{Z}_{n+1|n}$  with the following expression:

$$\widehat{\mathcal{B}}_{n+1|n}^{1-\alpha} = \text{Conv} \left( \bigcup_{b \in \mathcal{A}} G(\widehat{Z}_{n+1|n}^{(b)}) \right), \quad (17)$$

where  $G(Z) = \{(t, y) : y = Z(t), \forall t \in T\}$  is the graph of any function  $Z \in \mathcal{H}$  and  $\text{Conv}(\cdot)$  refers to the convex hull of the union of the graph of a collection of functions.

## 4. Experiments

The aim of this section is to illustrate and assess the performance of the proposed methodology in terms of prediction and inference in a simulated and real-world FTS. We compare against alternative approaches in the literature for both tasks: pointwise prediction and the construction of prediction bands. We assess the quality of the pointwise prediction using the root mean squared error. To evaluate the inferential performance we construct the simultaneous  $\text{PCB}_{1-\alpha}$  for different levels of nominal coverage  $1 - \alpha = \{0.8, 0.9, 0.95\}$  and then report the empirical coverage for each case. The average empirical coverage accounts for the average number of times that the function  $Z_{n+1}$  is covered by the band. While the empirical coverage gives insightful information, one can construct an arbitrarily



good band by sufficiently enlarge its amplitude (see comment below on how this may impact the calibration). Then, some notion of efficiency, is required in order to keep the bands as narrow as possible. In this sense, we report the amplitude of the band as a measure of its bandwidth,  $\text{Amp} = \int_T (U_{n+h}(t) - L_{n+h}(t))dt$ .

We test our proposed methodology (ARH-RKHS) against four prediction methods in the field. As simple baseline approaches we consider: the (historic) mean of the process  $\widehat{Z}_{n+1|n} = \hat{\mu}$ , and the predictor by persistence  $\widehat{Z}_{n+1|n} = Z_n$ . These naive predictors are associated to two limit cases of the ARH, that is, when the operator norm of  $\Psi$  is close to zero and one, respectively. As functional predictors we use the FAR estimation based in functional principal components (FPCA-FAR) as proposed in [Bosq \(2000\)](#) and implemented in the R-package ‘far’ [Julien et al. \(2015\)](#) and the Functional Partial Least Square Regression (FPLSR) [Delaigle et al. \(2012\)](#) already implemented in the R-package ‘ftsar’ [Hyndman et al. \(2020\)](#).

Two alternative methods are used to compare against our entropy procedure of functional predictive confidence bands, hereafter (fpcb). We consider two depth measures that allow to construct simultaneous confidence bands for a functional data set: the modified band depth (MBD) [López-Pintado and Romo \(2009\)](#) and the random projection depth (RPD) [Cuevas et al. \(2007\)](#), already implemented in the R-packages ‘depthTools’ [Lopez-Pintado and Torrente \(2013\)](#) and ‘fda-usc’ [Febrero-Bande and Oviedo de la Fuente \(2013\)](#) respectively. We also construct Gaussian and empirical pointwise bands which involve applying the usual Gaussian and empirical quantiles to the bootstrap pseudo-replicates  $\widehat{Z}^*$  at each point of the domain  $t \in T$ . Our proposal is implemented in the R-package ‘fpcb’ [Hernández et al. \(2021\)](#).

In what follows, we consider the Gaussian kernel function  $K(t, s) = \exp(-\sigma\|t - s\|^2)$  for the estimation of the ARH-RKHS. For both the prediction and inferential exercises all the hyperparameters are calibrated through grid search over a predefined temporal window dividing the sample for training and validation (the percentages are specified for each experiment). These hyperparameters are: the bandwidth parameter of the kernel, ( $\sigma$ ); the dimension of the basis function system ( $d$ ) of the ARH-RKHS; the functional principal components for the FPCA-FAR and FPLSR methods. The optimal parameter is the one that minimises a particular metric. In the prediction task this metric is the root mean square error and for the task of the  $\text{PCB}_{1-\alpha}$  construction the metric is the pinball loss (see [Koenker and Bassett Jr \(1978\)](#)). The number of bootstrap pseudo-replicates  $B$  is 1000 and remain fixed for all the numerical experiments. Finally, the assessment measures are computed on fresh samples out of the calibration time window.

The full procedure to construct the predictive confidence band construction can be summarized as follows:

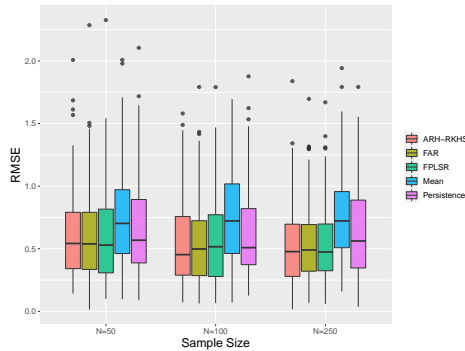
1. Given a raw functional time series data set  $Z_k$  and a kernel function  $K(s, t)$  we obtain the smoothed curves or functional approximation  $\tilde{Z}_k$ .
2. Estimate the model using Eq. 5 and Eq. 13 and obtain the fitted values  $\hat{Z}_k$ .
3. Following the bootstrap procedure, obtain the bootstrap predictive pseudo-replicates  $Z^* = \{Z_{n+h}^{(1)}, \dots, Z_{n+h}^{(B)}\}$  and project them onto the same multivariate space used for the estimation of the model in [2]
4. Solve the optimization problem in Eq. 16 and construct the  $\widehat{\mathcal{R}}_{1-\alpha}$  for a desired level of confidence, usually  $1 - \alpha = \{0.8, 0.9, 0.95\}$ .
5. Identify the predictive pseudo-replicates whose RKHS representation (the multivariate coefficients  $\hat{\mathbf{c}}^* \in \mathbb{R}^d$ ) belong to the  $\widehat{\mathcal{R}}_{1-\alpha}$  and construct the  $\text{PCB}_{1-\alpha}$ ,  $\widehat{\mathcal{B}}_{n+1|n}^{1-\alpha}$ , applying Eq. 17.

6. To measure the coverage of the band, check if  $G(Z_{n+h}) \in \hat{\mathcal{B}}_{n+1|n}^{1-\alpha}$ . –This step is only possible when testing data is available–.

#### 4.1. Monte Carlo simulation study

We generate raw functional time series coming from a FAR(1) process following the scheme presented in Eq. 5 using the `far` R package. We consider three scenarios with sample sizes  $N = \{50, 100, 250\}$  sampled at 64 equally spaced points in the interval  $T = [0, 1]$ . The finite dimension space in the simulation is of size  $m' = 5$  and we use a Fourier functional basis. While the simulation functionality is intrinsic to the package, we choose to adapt the time grid of the basis to coincide with the one used in the package `fda`. Although seemingly inoffensive, the default choice is less appropriate since it covers the extreme points of the grid (i.e.  $t = 0$  and  $t = 1$ ). We use the covariance and autoregression operators by default, which coincides with the ones in [Damon and Guillas \(2005\)](#), that is those defined by the following diagonal matrix representations  $\text{diag}(\Psi) = (0.45, 0.9, 0.34, 0.45)$  and  $\text{diag}(\Gamma_0) = (0.5, 0.23, 0.018)$ . The matrices are completed up to size  $m'$  with a decreasing perturbation (controlled by the quantity `eps = 0.05` in the package) to better approximate the behaviour of the corresponding linear operators. Notice that this simple structure of diagonal operators is beneficial to methods like FPLSR that copes independently the projected series of coefficients of the simulated process. To calibrate the hyperparameters of each model we divide the FTS into the usual training–validation fashion (80%–20%), and we simulate an extra curve to test the results. This procedure was embedded in a Monte Carlo study of 100 replicates.

In terms of the root mean square error shown in Figure 1a and Table 1b the ARH-RKHS presents a good performance among the functional methods, although the difference is not statistically significant. The Monte Carlo study exhibits the accuracy improves with the sample size, that is: as we have more information available the estimation error is reduced. Regarding the coverage, the `fpcb` method shows the best results in terms of empirical coverage through all the sample sizes considered. Moreover, with the proposed methodology the nominal coverage can be reached with  $N = 100$  for 80% and 90% and for  $N = 250$  for 80%, 90% and 95% of nominal coverage. These levels of empirical coverage are obtained with bands that are on average 12% wider than the MBD and RPD bands, and 80% wider than the pointwise bands.



(a) Monte Carlo Results: RMSE distribution by prediction method throughout a variation of the sample size from 50 to 250.

N	ARH-RKHS	FAR	FPLSR	Mean	Persistence
N=50	0.63 (0.376)	0.61 (0.371)	0.62 (0.402)	0.77 (0.419)	0.67 (0.403)
N=100	0.57 (0.349)	0.56 (0.342)	0.56 (0.347)	0.75 (0.375)	0.63 (0.364)
N=250	0.54 (0.338)	0.55 (0.329)	0.55 (0.325)	0.75 (0.369)	0.64 (0.372)

(b) Average RMSE by prediction method throughout a variation of the sample size ( $N$ ) from 50 to 250, (standard-error reported in parentheses); 100 MC replications.

Figure 1: Performance results of the Monte Carlo experiment.

Table 1: Monte Carlo Experiment: average coverage and amplitude for different nominal coverages ( $1 - \alpha$ ), band construction methods and sample sizes, (standard-error reported in parentheses); 100 MC replications.

Sample size	Method	Nominal 80%		Nominal 90%		Nominal 95%	
		Cov.	Amp.	Cov.	Amp.	Cov.	Amp.
N = 50	fpcb	<b>69%</b> (0.465)	3.09 (2.326)	<b>79%</b> (0.409)	4.04 (3.212)	<b>91%</b> (0.288)	5.75 (4.372)
	MBD	60% (0.492)	2.61 (1.713)	71% (0.456)	3.55 (2.561)	87% (0.338)	5.43 (4.099)
	RPD	60% (0.492)	2.59 (1.703)	71% (0.456)	3.58 (2.571)	84% (0.368)	5.32 (3.933)
	Gaussian	36% (0.482)	1.43 (1.075)	58% (0.496)	2.29 (2.033)	76% (0.429)	3.67 (3.007)
	Empirical	36% (0.482)	1.42 (1.073)	58% (0.496)	2.25 (1.903)	74% (0.441)	3.66 (2.968)
N = 100	fpcb	<b>84%</b> (0.368)	3.95 (2.381)	<b>87%</b> (0.338)	4.61 (2.782)	<b>93%</b> (0.256)	5.45 (3.026)
	MBD	76% (0.429)	3.30 (2.305)	83% (0.378)	4.29 (2.749)	92% (0.273)	5.18 (2.883)
	RPD	75% (0.435)	3.24 (2.162)	83% (0.378)	4.16 (2.642)	92% (0.273)	5.03 (2.743)
	Gaussian	63% (0.485)	1.81 (1.116)	75% (0.435)	2.55 (1.562)	91% (0.288)	3.47 (1.93)
	Empirical	62% (0.488)	1.79 (1.113)	74% (0.441)	2.54 (1.559)	90% (0.302)	3.45 (1.927)
N = 250	fpcb	<b>84%</b> (0.368)	3.43 (2.003)	<b>92%</b> (0.273)	5.40 (4.749)	<b>93%</b> (0.256)	24.46 (62.196)
	MBD	69% (0.465)	3.05 (1.883)	85% (0.359)	4.83 (3.705)	91% (0.288)	18.04 (42.118)
	RPD	66% (0.476)	2.94 (1.789)	84% (0.368)	4.68 (3.813)	90% (0.302)	18.54 (43.766)
	Gaussian	52% (0.502)	1.61 (0.959)	75% (0.435)	3.07 (2.838)	86% (0.349)	15.70 (39.327)
	Empirical	54% (0.501)	1.60 (0.954)	75% (0.435)	3.07 (2.868)	87% (0.338)	15.63 (39.074)

#### 4.2. Real-world data application

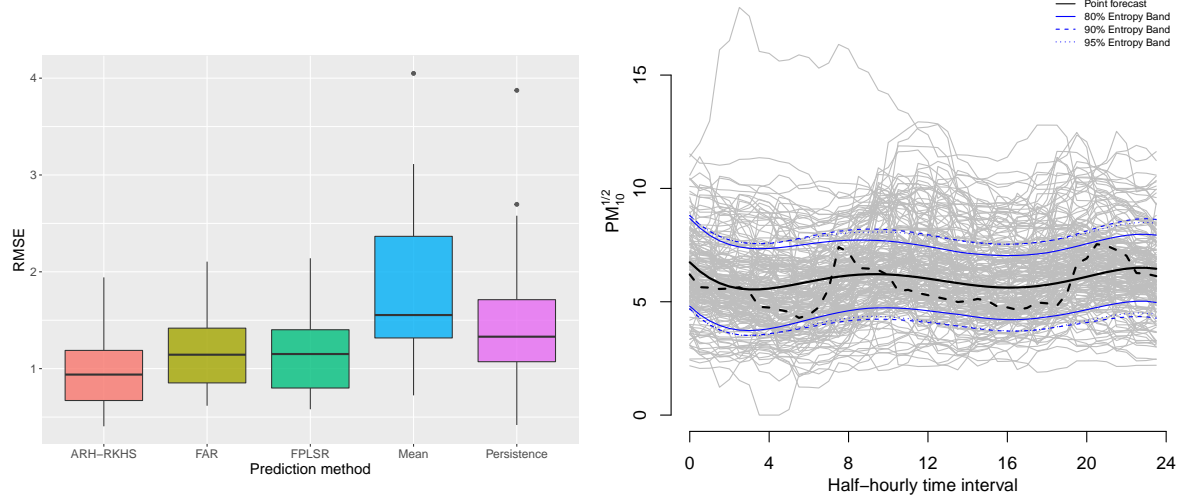
We illustrate our proposed methodology with the Particulate Matter Concentrations dataset available in R-package ‘`ftsa`’. The data consists of 182 curves that measure of the concentrations (measured in  $\mu\text{g}/\text{m}^3$ ) of particular matter with an aerodynamic diameter of less than 10 $\mu\text{m}$  (PM10) and half-hourly sampled and taken in Graz-Mitte, Austria from October 1, 2010 until March 31, 2011. A square root transformation is applied in order to stabilize the variance.

For this experiment we divide the sample in the usual training–validation–testing fashion (60%–20%–20%). Given the sample size we use 146 curves to train and validate the parameters and 36 curves for testing. This mean we have a forecasting horizon of 36 days with the respective predictive confidence bands. For this experiment the value of the kernel parameter  $\sigma$  is 1, and 7 basis functions were used for all the estimation methods. The results presented in Table 2 correspond to the average over all the forecast horizon.

The results are presented in Figure 2 and Table 2. In terms of the accuracy of the prediction methods it can be seen that our proposed model shows a lower RMSE, even if the difference among the functional methods is not statistically significant. However, any of the functional methods improve the quality of the forecast with respect to the persistence and historic mean prediction. The coverage and amplitude results show that the fpcb method offers solid results to make inference. In the three scenarios stated, the fpcb method achieves the desired nominal levels of confidence. This desired confidence level is obtained with wider bands; for a nominal coverage of 95% the fpcb method is, on average, 30% wider than the alternative procedures.

Finally, let us comment on the shape of the fpcb bands as illustrated in the right panel of Figure 2. The target function has a form presenting clearly two peaks which are usually associated to traffic rush in the morning and the afternoon. Notice that these peaks reflect the behaviour of economic and social patterns and are impacted by the calendar. That is, they may present shifts during the year, caused by time saving local rules and are more clear during working days than weekends. The prediction has a much smoother shape. Indeed, we aim to estimate the (non statistical) predictor  $\tilde{Z}_{n+1|n}$  since this is the best what can do with the information given until moment  $n$ . Naturally, the band we construct also inherits this constraint which explains the much smoother behaviour with respect to the datum  $Z_{n+1}$ .

Figure 2: PM10 data set: RMSE distribution by prediction method (left); fpcb predictive confidence bands for different confidence levels (instance  $h=27$ ) (right).



## 5. Concluding comments

In this paper we present a novel method to construct simultaneous confidence bands for the prediction of a functional time series data set, based on an entropy measure for stochastic processes. To construct predictive bands we use a functional version of residual bootstrap that allow us to estimate the prediction law through the use of pseudo-predictions. Each pseudo-realisation is then projected into a space of finite dimension, associated to a functional basis, where the  $1 - \alpha$  MES are obtained. We push back the minimum entropy set to the functional space and construct a band using the regularity of the RKHS. Throughout a Monte Carlo study, we show the performance of the proposed model in terms of the accuracy, coverage and amplitude, against other prediction methodologies and band construction techniques for functional time series. To illustrate the procedure through a real-world

Table 2: PM10 data set: average coverage and amplitude for different nominal coverages ( $1 - \alpha$ ), band construction methods and sample sizes, (standard-error reported in parentheses); forecast horizon = 36.

Method	Nominal 80%		Nominal 90%		Nominal 95%	
	Cov.	Amp.	Cov.	Amp.	Cov.	Amp.
Entropy	<b>86%</b> (0.351)	9.35 (5.079)	<b>92%</b> (0.28)	10.09 (5.53)	<b>94%</b> (0.232)	10.52 (5.541)
MBD	53% (0.506)	6.14 (3.242)	72% (0.454)	7.44 (4.02)	72% (0.454)	8.33 (4.529)
RPD	50% (0.507)	6.23 (3.354)	69% (0.467)	7.77 (4.015)	69% (0.467)	8.63 (4.541)
Gaussian	44% (0.504)	4.01 (2.141)	58% (0.5)	5.16 (2.755)	72% (0.454)	6.13 (3.236)
Empirical	39% (0.494)	3.92 (2.084)	58% (0.5)	5.15 (2.745)	72% (0.454)	6.22 (3.354)

data set, an example of particulate matter concentrations is presented. Our simulation study demonstrated that the entropy procedure offers a better coverage which improves (reaching in some cases the nominal value) as the sample sizes increases. For both numerical experiments our proposed method for the bands construction achieves a good compromise between coverage and efficiency, the latter measured through the bandwidth.

An important aspect of our method is the construction of the band using a convex hull, as defined in Eq. (17). This implies that the band is compact, leaving aside non-connected configurations. If that were the case, our construction would result on wider bands than the optimal ones. Of course, such situations may arise in practice, for instance if the functional time series presents different regimes or seasonal patterns. Indeed, these non linear or non stationary settings need more intrincated constructions that may be investigated in future work.

An important connection with more classical time series can be made. Actually, prediction on FTS can be viewed as simultaneous multi-step ahead prediction, even in the case where the one-step-ahead function is computed. Take for instance the case on section 4.2. Since each function covers 48 single time points, the FTS approach produces a simultaneous forecast for 48 different horizons. Then, our approach to compute prediction bands is easily adapted to the construction of prediction intervals simultaneously for several horizons. This is the case for instance in [Staszewska-Bystrova \(2011\)](#) where simultaneous prediction bands are constructed for the trajectories of an impulse-response effect on vector autoregressive processes. Also in [Wolf and Wunderli \(2015\)](#) the problem is studied from the perspective of joint prediction regions. A comparison of these approaches is given, within the framework of non linear and non stationary FTS in [Antoniadis et al. \(2016\)](#).

## Acknowledgments

NH acknowledge financial support from the Spanish Ministry of Economy and Competitiveness ECO2015-66593-P.

## References

- J. O. Ramsay, Functional data analysis, Wiley Online Library, 2006.
- D. Bosq, Linear processes in function spaces: theory and applications, volume 149, Springer Science & Business Media, 2000.

- S. Bonnevey, J. Cugliari, V. Granger, Predictive maintenance from event logs using wavelet-based features: an industrial application, in: *International Workshop on Soft Computing Models in Industrial and Environmental Applications*, Springer, 2019, pp. 132–141.
- A. Antoniadis, X. Brossat, J. Cugliari, J.-M. Poggi, A prediction interval for a function-valued forecast model: Application to load forecasting, *International Journal of Forecasting* 32 (2016) 939 – 947. doi:[10.1016/j.ijforecast.2015.09.001](https://doi.org/10.1016/j.ijforecast.2015.09.001).
- E. Paparoditis, H. L. Shang, Bootstrap prediction bands for functional time series, *arXiv preprint arXiv:2004.03971* (2020).
- S. Hörmann, P. Kokoszka, et al., Weakly dependent functional data, *The Annals of Statistics* 38 (2010) 1845–1884.
- A. Aue, D. D. Norinho, S. Hörmann, On the prediction of stationary functional time series, *Journal of the American Statistical Association* 110 (2015) 378–392. doi:[10.1080/01621459.2014.909317](https://doi.org/10.1080/01621459.2014.909317).
- J. Alvarez-Liévana, A review and comparative study on functional time series techniques, *arXiv preprint arXiv: 1706.06288* (2017).
- K. Nagbe, J. Cugliari, J. Jacques, Short-term electricity demand forecasting using a functional state space model, *Energies* 11 (2018) 1–24. doi:[10.3390/en11051120](https://doi.org/10.3390/en11051120).
- D. Wang, Z. Zhao, R. Willett, C. Y. Yau, Functional autoregressive processes in reproducing kernel hilbert spaces, *arXiv preprint arXiv:2011.13993* (2020).
- A. Antoniadis, E. Paparoditis, T. Sapatinas, A functional wavelet–kernel approach for time series prediction, *Journal of the Royal Statistical Society: Series B (Statistical Methodology)* 68 (2006) 837–857.
- R. J. Hyndman, H. L. Shang, Forecasting functional time series, *Journal of the Korean Statistical Society* 38 (2009) 199–211.
- A. Antoniadis, X. Brossat, J. Cugliari, J.-M. Poggi, Prévision d’un processus à valeurs fonctionnelles en présence de non stationnarités. application à la consommation d’électricité, *Journal de la Société Française de Statistique* 153 (2012) 52–78.
- D. Degras, Simultaneous confidence bands for the mean of functional data, *Wiley Interdisciplinary Reviews: Computational Statistics* 9 (2017) e1397.
- C. R. Genovese, L. Wasserman, Confidence sets for nonparametric wavelet regression, *The Annals of Statistics* 33 (2005) 698–729. doi:[10.1214/009053605000000011](https://doi.org/10.1214/009053605000000011).
- A. Delaigle, P. Hall, et al., Defining probability density for a distribution of random functions, *The Annals of Statistics* 38 (2010) 1171–1193.
- R. Fraiman, G. Muniz, Trimmed means for functional data, *Test* 10 (2001) 419–440.
- S. López-Pintado, J. Romo, On the concept of depth for functional data, *Journal of the American Statistical Association* 104 (2009) 718–734.



- A. Cuevas, M. Febrero, R. Fraiman, Robust estimation and classification for functional data via projection-based depth notions, *Computational Statistics* 22 (2007) 481–496.
- P. Galeano, E. Joseph, R. E. Lillo, The mahalanobis distance for functional data with applications to classification, *Technometrics* 57 (2015) 281–291.
- G. Martos, A. Muñoz, J. González, Generalizing the mahalanobis distance via density kernels, *Intelligent Data Analysis* 18 (2014) S19–S31.
- H. Cardot, P. Cénac, P.-A. Zitt, et al., Efficient and fast estimation of the geometric median in hilbert spaces with an averaged stochastic gradient algorithm, *Bernoulli* 19 (2013) 18–43.
- G. Martos, N. Hernández, A. Muñoz, J. M. Moguerza, Entropy measures for stochastic processes with applications in functional anomaly detection, *Entropy* 20 (2018) 33.
- R. J. Hyndman, Computing and graphing highest density regions, *The American Statistician* 50 (1996) 120–126.
- T. Hsing, R. Eubank, Theoretical foundations of functional data analysis, with an introduction to linear operators, John Wiley & Sons, 2015.
- A. Muñoz, J. González, Representing functional data using support vector machines, *Pattern Recognition Letters* 31 (2010) 511–516.
- F. Cucker, S. Smale, On the mathematical foundations of learning, *Bulletin of the American Mathematical Society* 39 (2002) 1–49.
- B. J Mercer, Xvi. functions of positive and negative type, and their connection the theory of integral equations, *Phil. Trans. R. Soc. Lond. A* 209 (1909) 415–446.
- A. Mas, B. Pumo, Linear processes for functional data, in: *The Oxford Handbook of Functional Data*, Oxford Univ. Press, 2011, pp. 47–71.
- J. Damon, S. Guillas, Estimation and simulation of autoregressive hilbertian processes with exogenous variables, *Statistical Inference for Stochastic Processes* 8 (2005) 185–204.
- A. Rényi, et al., On measures of entropy and information, in: *Proceedings of the Fourth Berkeley Symposium on Mathematical Statistics and Probability, Volume 1: Contributions to the Theory of Statistics*, The Regents of the University of California, 1961, pp. 547–561.
- A. Muñoz, J. Moguerza, Estimation of high-density regions using one-class neighbor machines, *IEEE Transactions on Pattern Analysis and Machine Intelligence* 28 (2006) 476–480.
- H. L. Shang, Bootstrap methods for stationary functional time series, *Statistics and Computing* 28 (2018) 1–10.
- E. Paparoditis, et al., Sieve bootstrap for functional time series, *The Annals of Statistics* 46 (2018) 3510–3538.
- Y. Chen, C. S. Pun, A bootstrap-based kpss test for functional time series, *Journal of Multivariate Analysis* 174 (2019) 104535.

- J. Franke, E. G. Nyarige, A residual-based bootstrap for functional autoregressions, arXiv preprint arXiv:1905.07635 (2019).
- L. Pascual, J. Romo, E. Ruiz, Bootstrap predictive inference for arima processes, *Journal of Time Series Analysis* 25 (2004) 449–465.
- D. Fresoli, E. Ruiz, L. Pascual, Bootstrap multi-step forecasts of non-gaussian var models, *International Journal of Forecasting* (2014).
- D. Julien, G. Serge, M. D. Julien, Package ‘far’, 2015.
- A. Delaigle, P. Hall, et al., Methodology and theory for partial least squares applied to functional data, *Annals of Statistics* 40 (2012) 322–352.
- R. J. Hyndman, H. L. Shang, M. H. L. Shang, Package ‘ftsa’, 2020.
- S. Lopez-Pintado, A. Torrente, depthtools: Depth tools package, 2013.
- M. Febrero-Bande, M. Oviedo de la Fuente, Package ‘fda. usc’: Functional data analysis and utilities for statistical computing, 2013.
- N. Hernández, J. Cugliari, J. Jacques, fpcb: Functional predictive confidence bands, 2021.
- R. Koenker, G. Bassett Jr, Regression quantiles, *Econometrica: journal of the Econometric Society* (1978) 33–50.
- A. Staszewska-Bystrova, Bootstrap prediction bands for forecast paths from vector autoregressive models, *Journal of Forecasting* 30 (2011) 721–735. doi:[10.1002/for.1205](https://doi.org/10.1002/for.1205).
- M. Wolf, D. Wunderli, Bootstrap joint prediction regions, *Journal of Time Series Analysis* 36 (2015) 352–376. doi:[10.1111/jtsa.12099](https://doi.org/10.1111/jtsa.12099).